ApoE isoform-specific regulation of regeneration in the peripheral nervous system

Human Molecular Genetics, 2011, Vol. 22, No. 12 **2406–2421**
doi:10.1093/hmg/ddr147
Advance Access published on April 8, 2011

ApoE isoform-specific regulation of regeneration in the peripheral nervous system

Laura H. Comley[1,2,†], Heidi R. Fuller[4,5,†], Thomas M. Wishart[1,2], Chantal A. Mutsaers[1,2], Derek Thomson[1,2], Ann K. Wright[1,2], Richard R. Ribchester[1,2], Glenn E. Morris[4,5], Simon H. Parson[1,2], Karen Horsburgh[3] and Thomas H. Gillingwater[1,2,*]

[1]Euan MacDonald Centre for Motor Neurone Disease Research, [2]Centre for Integrative Physiology and [3]Centre for Cognitive and Neural Systems, University of Edinburgh, Edinburgh EH8 9XD, UK, [4]Wolfson Centre for Inherited Neuromuscular Disease, RJAH Orthopaedic Hospital and [5]Institute for Science and Technology in Medicine, Keele University, Oswestry SY10 7AG, UK

Received March 2, 2011; Revised and Accepted March 30, 2011

Apolipoprotein E (apoE) is a 34 kDa glycoprotein with three distinct isoforms in the human population (apoE2, apoE3 and apoE4) known to play a major role in differentially influencing risk to, as well as outcome from, disease and injury in the central nervous system. In general, the apoE4 allele is associated with poorer outcomes after disease or injury, whereas apoE3 is associated with better responses. The extent to which different apoE isoforms influence degenerative and regenerative events in the peripheral nervous system (PNS) is still to be established, and the mechanisms through which apoE exerts its isoform-specific effects remain unclear. Here, we have investigated isoform-specific effects of human apoE on the mouse PNS. Experiments in mice ubiquitously expressing human apoE3 or human apoE4 on a null mouse apoE background revealed that apoE4 expression significantly disrupted peripheral nerve regeneration and subsequent neuromuscular junction re-innervation following nerve injury compared with apoE3, with no observable effects on normal development, maturation or Wallerian degeneration. Proteomic isobaric tag for relative and absolute quantitation (iTRAQ) screens comparing healthy and regenerating peripheral nerves from mice expressing apoE3 or apoE4 revealed significant differences in networks of proteins regulating cellular outgrowth and regeneration (myosin/actin proteins), as well as differences in expression levels of proteins involved in regulating the blood–nerve barrier (including orosomucoid 1). Taken together, these findings have identified isoform-specific roles for apoE in determining the protein composition of peripheral nerve as well as regulating nerve regeneration pathways *in vivo*.

INTRODUCTION

Genetic factors which influence the incidence and severity of neurological conditions are the subject of intensive research, as they offer the possibility of better prognostic/diagnostic tools as well as the prospect of identifying novel therapeutic approaches. One genetic factor that is a well-known modifier of disease onset and progression in the central nervous system (CNS) is apolipoprotein E (apoE). ApoE is a 34 kDa glycoprotein and is a major determinant of lipid transport and metabolism. There are three distinct isoforms present in humans: apoE2, apoE3 and apoE4. Of these, apoE4, which is present in one-third of the population, is most commonly associated with an increased risk of neurodegeneration in the CNS (1,2). It is well established that apoE4 is a major risk factor for Alzheimer's disease (3–5) as well as several other neurodegenerative conditions, including Parkinson's disease (6,7). Similarly, apoE4 is associated with a poor outcome after traumatic brain injury, stroke and intracranial haemorrhage (8–12). Conversely, apoE3 has been shown to attenuate CNS degeneration in conditions such as Wilson's disease (13).

Although the influence of apoE genotype on CNS injury and disease is well established, there is only a partial understanding of any potential influence of apoE genotype on the

*To whom correspondence should be addressed. Tel: +44 1316503724; Fax: +44 1316504193; Email: t.gillingwater@ed.ac.uk
†The authors wish it to be known that, in their opinion, the first two authors should be regarded as joint First Authors.

peripheral nervous system (PNS) (14,15). This lack of knowledge is rather surprising given that ApoE is expressed throughout the PNS, including at the neuromuscular junction (NMJ) (16,17), where expression levels dramatically increase in response to nerve crush injury and exposure to harmful environmental stimuli (18–20). Although an association between apoE genotype and disease outcome has been demonstrated for human patients with diabetic neuropathies (21,22), the influence of apoE genotype on other human PNS disorders—such as motor neuron disease—remains controversial (23–32). Previous studies using genetically modified animals to examine degeneration and regeneration in the PNS have only investigated the effects of complete loss of apoE expression (33,34), rather than the more biologically relevant question of the influence of the apoE isoform.

Similarly, the underlying mechanisms through which different apoE isoforms differentially affect the nervous system remain unclear. New experimental approaches to explore the mechanisms through which apoE influences the nervous system are therefore required. The PNS offers an ideal, experimentally accessible model system with which to study the influence of apoE isoforms on a variety of *in vivo* processes, including development, maturation, degeneration and regeneration.

Here, we have used mouse models to compare the consequences of human apoE3 and human apoE4 expression on the form, function and molecular composition of the healthy and degenerating PNS.

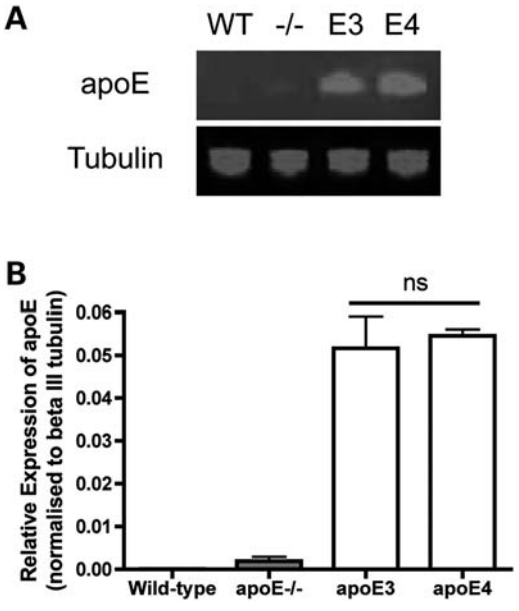

Figure 1. ApoE3 and apoE4 isoforms are expressed at equivalent levels in apoE3 and apoE4 transgenic mice. (**A**) Representative fluorescent western blot for apoE protein in the uninjured sciatic nerve of WT, apoE$^{-/-}$ ($-/-$), apoE3 (E3) and apoE4 (E4) mice. (**B**) Bar chart (mean ± SEM) showing quantification of apoE expression levels normalized to beta III tubulin loading control, confirming no difference in expression levels between apoE3 and apoE4 ($P > 0.05$, apoE3 versus apoE4; one-way ANOVA with Tukey's *post hoc* test; $n = 3$ for each genotype; ns, not significant).

RESULTS

ApoE4 significantly delays nerve regeneration and neuromuscular re-innervation following peripheral nerve injury

Previous studies reported that complete loss of apoE had no effect on nerve regeneration in the mouse PNS, following nerve injury (33,34). However, the more biologically relevant question of whether apoE3 or apoE4 can influence regeneration and neuromuscular re-innervation in the PNS was not addressed. We therefore set out to examine the influence of apoE genotype on regeneration in the PNS, using established transgenic mice expressing human apoE3 or apoE4 on a null mouse apoE background [apoE$^{-/-}$;apoE3 and apoE$^{-/-}$; apoE4; see Materials and Methods and reference (35)]. ApoE2 mice were not used for this study, as they express apoE at levels much higher than the apoE3 or apoE4 mice (35); thus, it would have been impossible to determine whether any effects observed were due to the genotype or were simply occurring due to differences in expression levels of apoE.

First, it was important to determine that apoE was expressed at similar levels in the transgenic lines used, to ensure that any differences observed were not due to a relative overexpression of one isoform. We therefore examined apoE expression levels in tibial nerves from apoE$^{-/-}$;apoE3 and apoE$^{-/-}$;apoE4 mice expressing human apoE3 or apoE4 and compared them with samples from wild-type (WT) mice and apoE$^{-/-}$ mice. As expected (9,35), apoE protein was undetectable in peripheral nerves from WT mice and apoE$^{-/-}$ mice [endogenous apoE is only expressed at low levels in the nervous system (9)]. However, apoE protein was generated from the human apoE3 and apoE4 transgenes in the peripheral nerve and was expressed at near-identical levels in nerves from apoE3 and apoE4 mice (Fig. 1).

We then quantified axon regeneration in the tibial nerve of apoE3 and apoE4 mice at 2 and 3 weeks following sciatic nerve injury (Fig. 2). At 1 week post-injury (the period when regeneration is beginning following the completion of Wallerian degeneration *in vivo*: see what follows), there was no difference in the numbers of axons in the sciatic nerve from apoE3 and apoE4 mice. However, at 2 weeks post-injury, apoE4 mice showed a significant reduction in the numbers of regenerating axons in the sciatic nerve compared with apoE3 mice (63% regeneration compared with apoE3 mice; $P < 0.05$; Fig. 2). This significant delay in regeneration was also present in apoE4 mice 3 weeks after injury, where regeneration was virtually complete in apoE3 mice, but had only reached 70% of apoE3 levels in apoE4 mice ($P < 0.05$; Fig. 2).

To confirm that the delay in axon regeneration observed in apoE4 mice subsequently resulted in impaired functional re-innervation of peripheral targets by regenerating axons, we quantified re-innervation of NMJs in the lumbrical muscles (innervated by the tibial nerve) of apoE3 and apoE4 mice after tibial nerve injury. At 2 weeks following nerve injury, lumbrical muscles in apoE4 mice had a significantly reduced number of re-innervated endplates compared with apoE3 mice (Fig. 3). We used fluorescent quantitative western blotting to establish that the delay in axon regeneration and neuromuscular re-innervation observed in apoE4

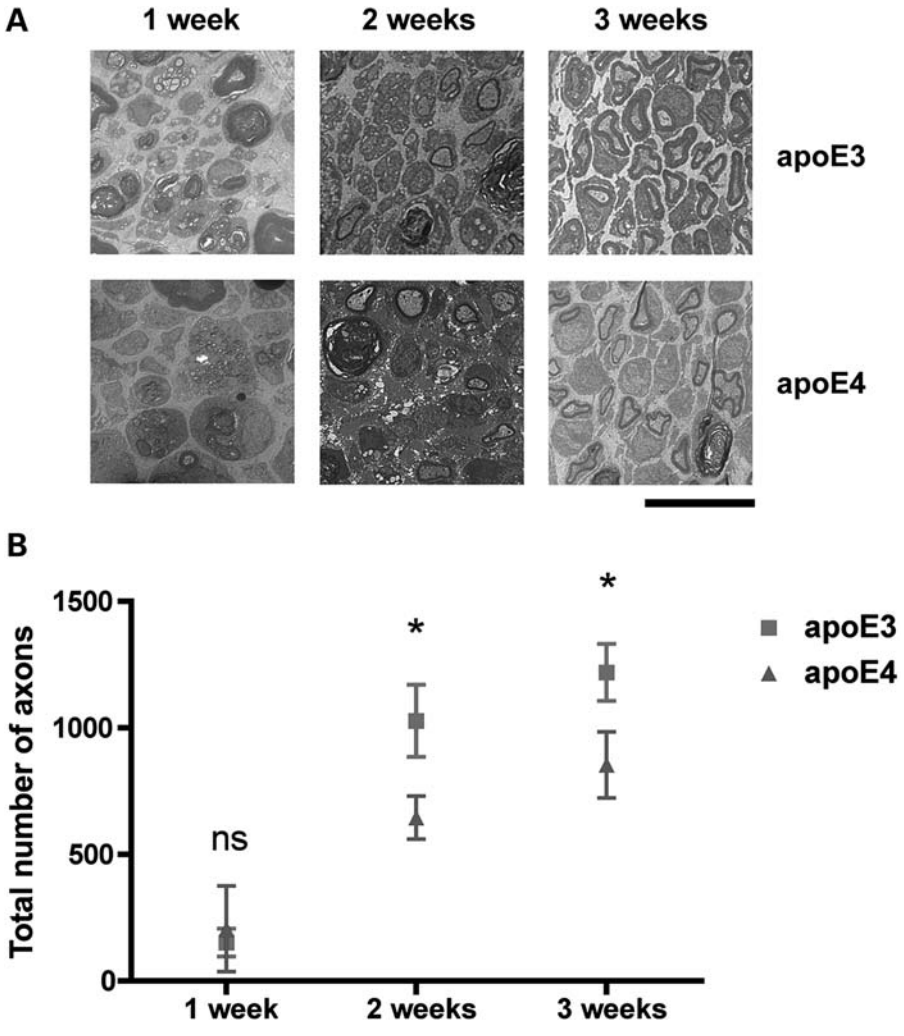

Figure 2. ApoE4 significantly impairs nerve regeneration following sciatic nerve injury. (**A**) Representative electron micrographs of cross-sections from adult sciatic nerves in apoE3 (E3) and apoE4 (E4) mice,1, 2 and 3 weeks after sciatic nerve crush. Scale bar = 10 μm. (**B**) Scatter plot (mean ± SEM) showing time course of axonal regeneration in apoE3 and apoE4 sciatic nerves following sciatic nerve crush. At both 2 and 3 weeks post-crush, apoE4 significantly delays regeneration (63 and 70% that of the levels of apoE3 axon regeneration at the same time points, respectively. 1 week, $P > 0.05$; *t*-test, two-tailed; apoE3, $n = 3$; apoE4, $n = 2$. 2 weeks, $P < 0.05$; *t*-test, two-tailed; apoE3, $n = 6$; apoE4, $n = 6$. 3 weeks, $P < 0.05$; *t*-test, two-tailed; apoE3, $n = 11$; apoE4, $n = 11$).

mice was not occurring due to differing expression levels of human apoE transgenes after nerve injury. Expression levels of apoE protein were identical in tibial nerves from apoE3 and apoE4 mice 2 weeks after nerve crush (Supplementary Material, Fig. S1). Taken together, these data show that apoE4 selectively delays nerve regeneration in the PNS.

ApoE genotype has no effect on normal form or function of the mouse PNS

To determine that the effects on regeneration were not occurring as an indirect result of pre-existing changes in the form or function of the uninjured PNS induced by different apoE genotypes, we next examined neuronal morphology and function in uninjured nerves and muscles from apoE3 and apoE4 mice and compared them with apoE$^{-/-}$ and WT mice. No qualitative or quantitative differences were observed in the morphology of the sciatic nerve or NMJs between mice of different genotypes (Fig. 4). Similarly, electrophysiological measurements from apoE4 mice suggested normal neuromuscular synaptic function in mice expressing a human apoE transgene: there were no effects on the rise time, amplitude or decay time of evoked endplate potentials (EPPs) and no discernible effect on miniature endplate potential (mEPP) frequency, amplitude or time course (Fig. 4). Developmental synaptic plasticity in the PNS was also unaltered in the presence of human apoE protein (Supplementary Material, Fig. S2). Thus, expression of either human apoE3 or apoE4 had no detrimental effect on the form, function or development of the uninjured mouse PNS.

ApoE genotype does not significantly delay Wallerian degeneration of axons or synapses following peripheral nerve injury

As apoE4 has been shown to modulate neurodegenerative events in the CNS (9,36–38), we next asked whether the presence of apoE3 or apoE4 influenced the rate of re-innervation

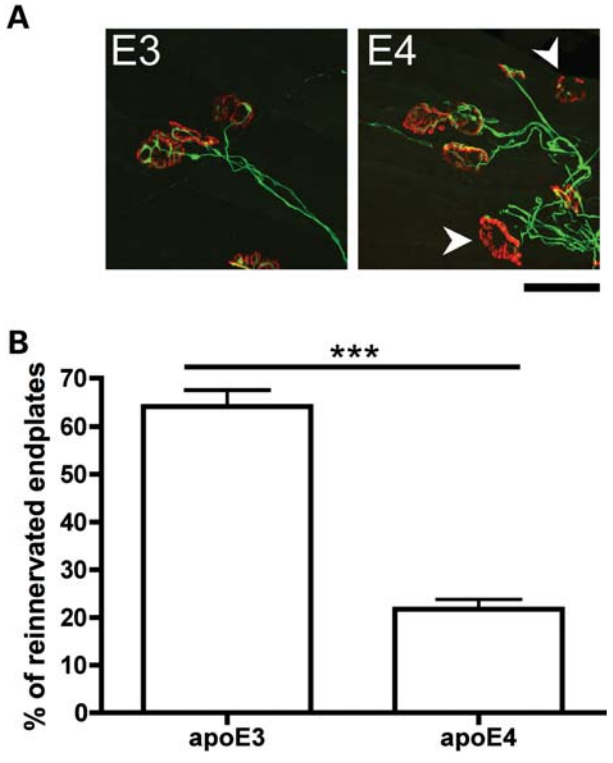

Figure 3. ApoE4 significantly impairs neuromuscular re-innervation following nerve crush injury in the mouse PNS. (**A**) Representative confocal micrographs showing immunohistochemically labelled NMJs from apoE3 and apoE4 lumbrical muscles 2 weeks after a tibial nerve crush. Pre-synaptic axons and motor nerve terminals are shown in green and post-synaptic acetylcholine receptors labelled with α-BTX are shown in red. Note how the apoE3 endplates have all been re-innervated, whereas some apoE4 endplates are still vacant and awaiting re-innervation (white arrows) at the same time-point. Scale bar = 30 μm. (**B**) Bar chart (mean ± SEM) showing levels of neuromuscular re-innervation in lumbrical muscles 2 weeks after a tibial nerve crush. Re-innervation was significantly impaired in apoE4 mice compared with apoE3 mice ($P < 0.001$; Mann–Whitney test, two-tailed; apoE3, $n = 5$ mice; apoE4, $n = 5$ mice).

by affecting the prior process of degeneration in the PNS, which is an essential pre-requisite for re-innervation. The extent of Wallerian degeneration occurring at NMJs in lumbrical muscles 24 h after tibial nerve cut injury was identical in apoE3 and apoE4 (Fig. 5A), similar to previous descriptions of Wallerian degeneration in WT mice (39,40). Likewise, Wallerian degeneration of axons in the sciatic nerve 1 week after nerve crush occurred identically in apoE3 and apoE4 mice (Fig. 5B and C). Thus, apoE genotype did not significantly delay Wallerian degeneration in the PNS, confirming that the impaired regeneration phenotype observed in apoE4 mice was occurring solely as a result of apoE4 directly modulating regeneration pathways in the peripheral nerve.

ApoE genotype modifies expression levels of proteins associated with cellular outgrowth and blood–nerve barrier integrity in peripheral nerve

Given our finding that apoE genotype selectively modifies nerve regeneration in the PNS, we next set out to identify potential molecular mechanisms regulating apoE-specific responses in the PNS *in vivo*. First, we used an iTRAQ (isobaric tag for relative and absolute quantitation) proteomic approach to compare protein expression levels in uninjured tibial nerve preparations from apoE3 and apoE4 mice ($n = 9$ mice per genotype, pooled into three independent samples per genotype). Importantly, it should be noted that these initial proteomic experiments were designed to detect changes in the peripheral nerve proteome occurring solely as a result of the presence of different isoforms of apoE, in the absence of any other external stimuli (e.g. nerve degeneration or regeneration). It should also be noted that our peripheral nerve preparations contained all of the cell types and tissues present in the peripheral nerve (e.g. not just axons of neurons but also glial cells, capillaries, extracellular matrix, etc.). These non-neuronal cells and tissues are important to consider in such experiments, as they play a key role in establishing a local microenvironment conducive to nerve regeneration.

Only proteins identified with >95% total ion score confidence intervals and by two or more unique peptides were accepted as being robust and reliable enough for inclusion in our analysis. Using this approach, 62 proteins showed increased expression levels >20% in uninjured peripheral nerves from apoE4 mice compared with apoE3 peripheral nerves (Table 1), and 40 proteins had decreased expression levels >20% in apoE4 peripheral nerves (Table 2). Note that neither of the protein products from the apoE3 or apoE4 transgenes was present on the tables of changed proteins as they are both human proteins and the analysis software was set to identify only mouse proteins. It should also be noted that, although the protein identifications were statistically significant (i.e. detected with two or more peptides and total ion scores of >95% confidence intervals), it was not always possible to distinguish between closely related protein isoforms (e.g. of myosin) unless proteotypic peptides (i.e. peptides that were entirely unique in sequence to that isoform) were detected. Thus, it is possible that specific isoforms of a protein (e.g. myosin) identified in this study may actually represent another closely related isoform in addition to, or in place of, the isoform actually listed.

Systems level analysis of protein expression changes using Ingenuity Pathway Analysis (IPA) software (see Materials and Methods) revealed potential changes in protein interaction networks associated with the regulation of tissue and cell morphology (based around interactions of myosin and actin proteins; Supplementary Material, Fig. S3A) and haematological regulation (including integrity of the blood–brain barrier (BBB)/blood–nerve barrier (BNB); Supplementary Material, Fig. S3B) in apoE4 mice. Taken together, these data show that expression of different apoE isoforms leads to significant modifications in the peripheral nerve proteome, even in the absence of injury or disease.

Given that these initial proteomic experiments were designed to detect changes in the peripheral nerve proteome occurring solely as a result of the presence of different isoforms of apoE, it was interesting to note numerous changes in expression levels of several myosin proteins that contribute to myosin/actin interaction networks in apoE4 mice, in the absence of any changes in corresponding actin proteins. Myosin proteins contributing to myosin/actin networks are

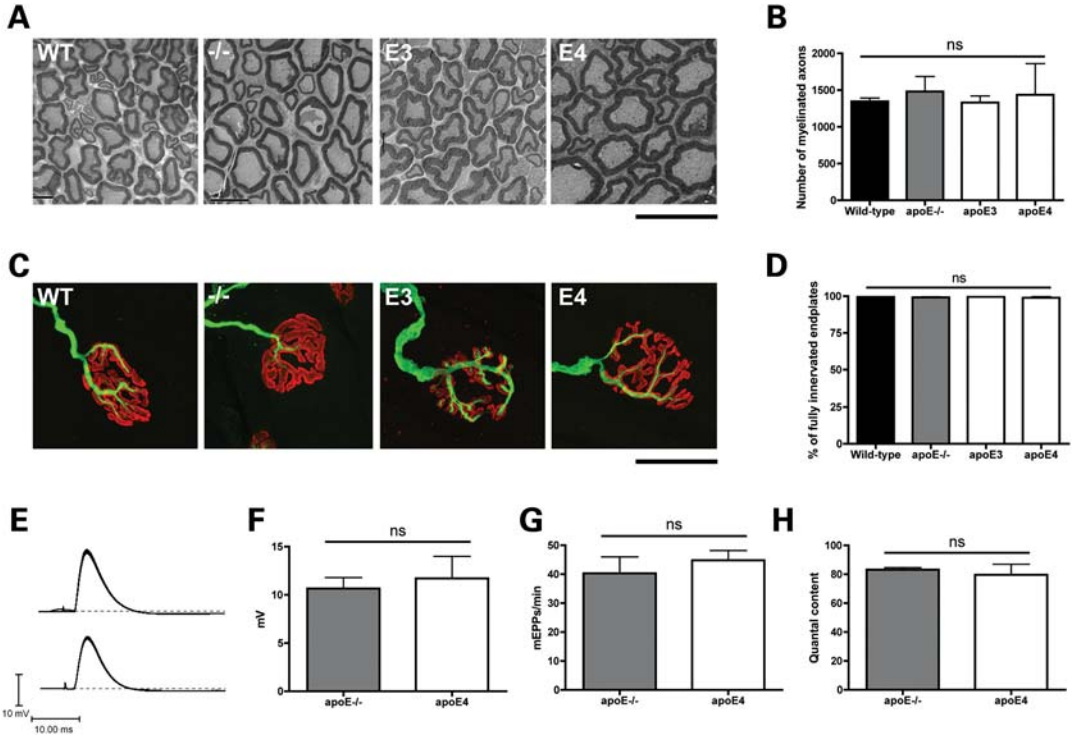

Figure 4. Expression of human apoE has no effect on normal axonal or neuromuscular form or function. (**A**) Representative electron micrographs of cross-sections from adult sciatic nerves in WT, apoE$^{-/-}$ (−/−), apoE3 (E3) and apoE4 (E4) mice. All genotypes had healthy myelinated axon profiles. Scale bar = 10 μm. (**B**) Bar chart (mean ± SEM) showing no significant difference in the number of myelinated axons in WT, apoE$^{-/-}$, apoE3 and apoE4 mice ($P > 0.05$; one-way ANOVA with Tukey's *post hoc* test; WT, $n = 3$; apoE$^{-/-}$, $n = 5$; apoE3, $n = 5$; apoE4, $n = 3$). (**C**) Representative confocal micrographs showing immunohistochemically labelled NMJs in LAL muscles showing mono-innervated, fully occupied endplates (i.e. 'normal' morphology) in WT, apoE$^{-/-}$ (−/−), apoE3 (E3) and apoE4 (E4) mice. More than 98% of NMJs in all muscles examined, regardless of genotype, showed these morphological characteristics. Pre-synaptic axons and motor nerve terminals are shown in green and post-synaptic acetylcholine receptors labelled with α-BTX are shown in red. Scale bar = 30 μm. (**D**) Bar chart (mean ± SEM) showing no significant difference in the percentage of fully occupied, mono-innervated WT, apoE$^{-/-}$, apoE3 and apoE4 mice ($P > 0.05$; Kruskal–Wallis test with Dunn's *post hoc* test; WT, $n = 8$; apoE$^{-/-}$, $n = 7$; apoE3, $n = 7$; apoE4, $n = 7$). (**E**) apoE$^{-/-}$ and apoE4 mice both showed robust EPPs in the FDB muscle in response to tibial nerve stimulation. (**F**) There was no significant difference in the amplitude of EPPs between apoE$^{-/-}$ and apoE4 mice. ($P > 0.05$; *t*-test, two-tailed; apoE$^{-/-}$, $n = 73$ fibres, $n = 3$ mice; apoE4, $n = 75$ fibres, $n = 3$ mice). (**G**) Muscles from both genotypes showed spontaneous mEPPs at an equivalent rate ($P > 0.05$; *t*-test, two-tailed; apoE$^{-/-}$, $n = 78$ fibres, $n = 3$ mice; apoE4, $n = 80$ fibres, $n = 3$ mice). (**H**) There was no significant difference in quantal content between apoE$^{-/-}$ and apoE4 mice ($P > 0.05$; *t*-test, two-tailed; apoE$^{-/-}$, $n = 48$ fibres, $n = 3$ mice; apoE4, $n = 32$ fibres, $n = 3$ mice). ns, not significant.

responsible for delivering the actin scaffold to relevant parts of the cell during periods of cell growth or reorganization, but concomitant changes in actin levels would be essential for the pathway to modify cell morphology (41–43). These findings were therefore consistent with our morphological data from the uninjured PNS, showing that apoE4 expression did not affect the normal form or function of the PNS, as might have been expected had actin protein levels also been altered. However, the changes we observed in myosin proteins in uninjured apoE4 nerves may represent a 'priming' response that does not result in any overt phenotype, but which could conceivably influence actin dynamics in response to stimuli inducing cell remodelling (e.g. peripheral nerve regeneration following nerve injury).

To test whether modifications in *both* actin and myosin components of myosin/actin interaction networks were consequently modified in regenerating peripheral nerves from apoE4 mice, we repeated our iTRAQ proteomic experiments using regenerating tibial nerves from apoE3 and apoE4 mice 3 weeks after nerve crush injury ($n = 9$ mice per genotype, pooled into three independent samples per genotype). As in our experiments on unlesioned nerves, there were large numbers of proteins with altered expression in regenerating nerves from apoE4 mice compared with apoE3 mice (Tables 3 and 4). Many of these proteins were similar to those changed in unlesioned nerves, including proteins involved in haematological regulation (e.g. haptoglobin and orosomucoid 1). However, even more marked changes were observed in expression levels of both myosin and actin proteins (Table 4). These findings were supported by systems level analysis: 55% of total proteins in one single myosin/actin interaction network had altered expression in uninjured nerves (Supplementary Material, Fig. S3A), whereas 83 and 86% of proteins contributing to two myosin/actin networks had modified expression levels in regenerating apoE4 nerves (Supplementary Material, Fig. S4A and B). Given the importance of myosin/actin pathways in driving cellular reorganization required for processes such as regeneration (41–43), the widespread reductions in expression of key proteins contributing to these networks in the apoE4 peripheral nerve are likely to play a significant role in reducing their regenerative capacity.

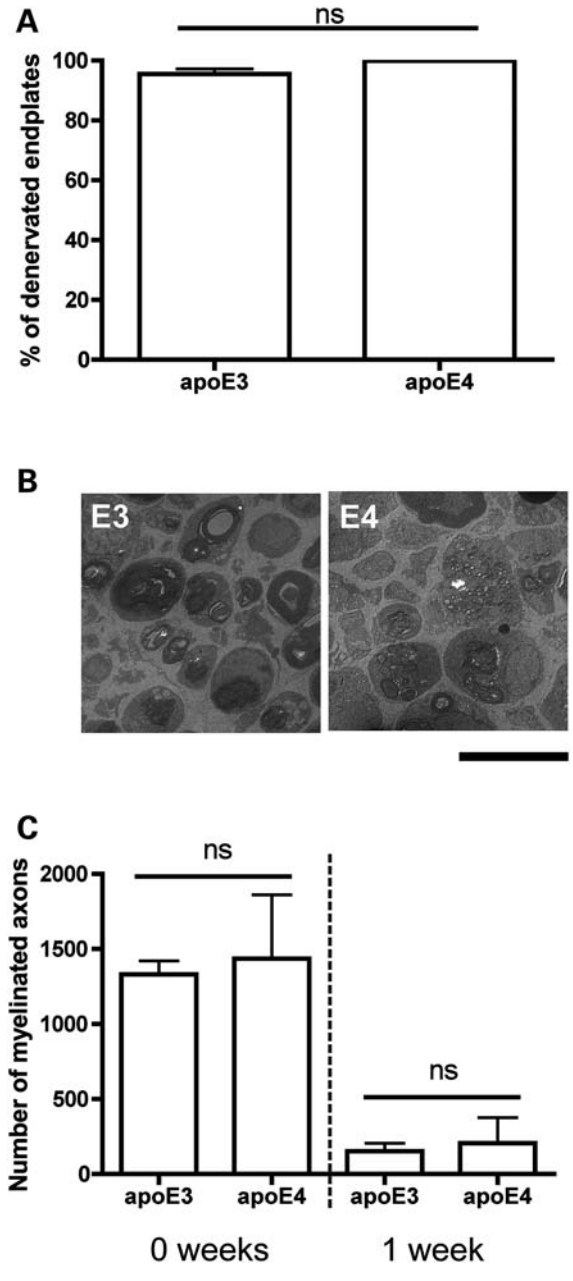

Figure 5. Wallerian degeneration of NMJs and axons following peripheral nerve crush injury occurs identically in apoE3 and apoE4 mice. (**A**) Bar chart (mean ± SEM) showing no significant difference between the percentage of denervated endplates observed in apoE3 and apoE4 lumbrical muscles 24 h after tibial nerve crush ($P > 0.05$; Mann–Whitney test, two-tailed; apoE3, $n = 5$; apoE4, $n = 3$ mice). (**B**) Representative electron micrographs of cross-sections from adult sciatic nerves in apoE3 (E3) and apoE4 (E4) mice 1 week after sciatic nerve crush. Scale bar = 10 μm. (**C**) Bar chart (mean ± SEM) showing reduced numbers of myelinated axons in apoE3 and apoE4 sciatic nerves 1 week after nerve crush injury (0 and 1 weeks: $P > 0.05$; one-way ANOVA with Tukey's *post hoc* test; 0 week: apoE3, $n = 5$; apoE4, $n = 3$. 1 week: apoE3, $n = 3$ mice; apoE4, $n = 2$).

DISCUSSION

In this study, we have demonstrated apoE genotype-dependent regulation of nerve regeneration in the PNS and used this finding to examine molecular mechanisms underlying deficient neurite outgrowth in peripheral nerves expressing apoE4. We showed that the presence of apoE4 selectively delays nerve regeneration and neuromuscular re-innervation compared with mice expressing apoE3, in the absence of any significant effects on the form, function, degeneration or developmental plasticity of the PNS. Comparative iTRAQ proteomics revealed concomitant significant changes to the proteome of the peripheral nerve in apoE4 mice, compared with that in apoE3 mice, with modified expression levels of proteins that contribute to the regulation of cellular outgrowth and regeneration (based around myosin/actin interactions) and haematological regulation (e.g. of the BNB).

The most notable phenotypic observation in the current study was a significant and selective impairment of nerve regeneration and neuromuscular re-innervation in the PNS of apoE4 mice following peripheral nerve injury. These data from the PNS are in agreement with previous *in vitro* studies of neurons from the CNS, showing that neurite outgrowth can be inhibited by apoE4 (44–46) and that intrinsic neuronal repair mechanisms are compromised in the presence of apoE4 in response to CNS injury (47). Our finding that apoE4 influences regenerative processes in the PNS also provides a possible explanation for several previous human cohort studies reporting associations between apoE genotype and progressive diseases of the PNS, including diabetic and HIV-associated neuropathies (21,22,48) and motor neuron disease. For the latter, there have been a number of human cohort studies investigating a possible relationship between the apoE4 allele and motor neuron disease, with conflicting results (23–29,31,32). Motor neuron regeneration has been shown to play a significant role in amyotrophic lateral sclerosis (ALS): as some motor neurons degenerate, leaving denervated muscle fibres, others sprout in an attempt to re-innervate vacant motor endplates and prolong muscle function (49). The findings reported here suggest that possession of the apoE4 allele could impact on disease progression in conditions such as ALS, as neurons in patients with apoE4 may have a reduced capacity for sprouting and re-innervation. Thus, knowledge of the apoE genotype status of individual human patients with peripheral nerve trauma or disease may provide valuable insights into the likelihood of success of regenerative events in the PNS and hence help to inform the likely rate of recovery or decline (15).

Our proteomic experiments revealed a significant influence of apoE genotype on the peripheral nerve proteome, both in uninjured nerves and in regenerating nerves. The limitations of this approach mean that we could only detect changes in global expression levels rather than gaining insights into more dynamic cellular processes (e.g. changes in subcellular localization and/or modified binding activity of specific or groups of proteins). However, our experiments did reveal changes in expression levels of a range of different myosin and actin proteins. Importantly, as we identified modified expression levels for a large number of myosin isoforms in uninjured nerves from apoE4 mice, it is possible to conclude that apoE4-mediated disruptions in myosin/actin networks were occurring as a direct consequence of the apoE genotype, and not simply as a result of impaired nerve regeneration in apoE4 mice. It has long been known that dynamic regulation of the actin cytoskeleton is a key regulator of cell morphology

Table 1. iTRAQ identification of proteins with >20% increased expression and peptide count >1 in the unlesioned sciatic nerve from ApoE4 mice compared with ApoE3 mice

Protein name	Accession number	Protein MW	Protein PI	Peptide count	Total ion score, CI percentage	Best ion score	Average ratio (E4/E3)	Standard deviation (E4/E3)
Haptoglobin precursor	8850219	42455.7	5.9	7	100.00	67.94	3.39	1.42
Orosomucoid 1	15215270	26393.8	5.4	5	100.00	58.65	2.05	0.53
Myomesin 2	170763465	179757.5	5.6	11	100.00	72.44	1.80	0.35
PK-120 precursor	2739028	112522.4	6.1	2	100.00	52.16	1.67	0.03
Myosin, heavy polypeptide 4, skeletal muscle	67189167	254149.5	5.6	85	100.00	127.38	1.67	0.44
Haemopexin precursor	160358829	55053.3	7.9	15	100.00	95.47	1.63	0.42
Muscle glycogen phosphorylase	6755256	104509.5	6.7	18	100.00	93.56	1.63	0.33
Myosin-binding protein C, fast type	81910387	143381.3	6.0	10	100.00	100.37	1.62	0.49
ATPase, Ca^{++} transporting, ubiquitous	74215005	116671.4	5.5	2	100.00	48.16	1.61	0.09
Major urinary protein	295910	22495.3	4.9	3	100.00	85.86	1.59	0.23
Major urinary protein	13276755	22609.4	5.0	3	100.00	85.86	1.58	0.21
MUP	755765	17535.8	4.9	2	100.00	62.95	1.53	0.12
Myh7 protein	187956918	252607.1	5.6	20	100.00	91.72	1.51	0.56
Alpha cardiac myosin heavy chain	191618	253883.5	5.6	18	100.00	91.72	1.48	0.58
Muscle creatine kinase	6671762	48101.2	6.6	14	100.00	101.99	1.45	0.34
S100 calcium binding protein A9 (calgranulin B)	6677837	14907.5	6.6	2	100.00	69.01	1.45	0.09
Solute carrier family 4 (anion exchanger), member 1	74138529	108215.2	5.4	2	100.00	50.97	1.45	0.01
Fibrinogen, gamma polypeptide	74143561	55480.4	5.4	6	100.00	84.66	1.43	0.09
Titin	123232572	3312853.3	6.2	2	100.00	37.84	1.43	0.05
Fibrinogen beta chain precursor	33859809	60169.0	6.7	12	100.00	78.56	1.41	0.29
Myosin, heavy polypeptide 8, skeletal muscle, perinatal	71143152	253848.8	5.7	46	100.00	106.43	1.40	0.58
Parvalbumin	31980767	14372.8	5.0	5	100.00	88.79	1.40	0.19
Myosin, heavy polypeptide 8, skeletal muscle, perinatal	187956525	253835.8	5.7	46	100.00	106.43	1.39	0.57
Haemoglobin, beta adult major chain	31982300	17513.4	7.1	13	100.00	107.43	1.36	0.22
Clusterin precursor	214010170	56451.5	5.5	4	100.00	82.73	1.36	0.47
mCG18455	148678485	256334.6	5.5	22	100.00	84.80	1.36	0.71
Troponin T	2340048	34082.0	9.4	4	100.00	78.26	1.35	0.16
Haemoglobin alpha, adult chain 2	145301549	16878.0	8.0	9	100.00	101.60	1.35	0.25
ATPase, Ca^{++} transporting, cardiac muscle, fast twitch 1	148685412	116243.4	5.3	12	100.00	114.25	1.35	0.24
Actinin alpha 3	7304855	110400.7	5.3	34	100.00	112.37	1.34	0.46
Phosphofructokinase, muscle	13529638	92278.8	8.2	8	100.00	67.00	1.34	0.11
Collagen, type VI, alpha 1 precursor	6753484	117555.5	5.2	7	100.00	91.16	1.33	0.17
Glutamine synthetase	31982332	45842.4	6.6	2	100.00	67.62	1.33	0.04
Myomesin 1 isoform 2	145279198	194032.5	6.0	7	100.00	81.84	1.33	0.13
Sarcalumenin, isoform CRA_a	148664814	59761.7	6.2	4	100.00	60.15	1.31	0.25
ATPase, Ca^{++} transporting, slow twitch 2 isoform a	158635979	124907.5	5.2	5	100.00	68.51	1.31	0.33
Histone cluster 1, H1c	9845257	29755.8	11.0	2	100.00	75.68	1.30	0.17
mCG2006, isoform CRA_a	148680420	187536.8	6.3	2	100.00	60.73	1.30	0.12
Glycogen phosphorylase, liver form	20178036	107417.7	6.6	5	100.00	58.28	1.29	0.20
Phosphoglycerate mutase 2	9256624	31972.9	8.7	8	100.00	89.17	1.29	0.17
Enolase 3, beta muscle, isoform CRA_a	148680653	54402.9	6.8	15	100.00	112.63	1.28	0.28
Sorbitol dehydrogenase	22128627	42431.2	6.6	2	100.00	54.45	1.28	0.23
RIKEN cDNA 1810020D17, isoform CRA_c	148684357	17880.5	7.8	2	100.00	44.25	1.27	0.04
Unnamed protein product	26345578	19080.7	10.5	3	100.00	67.62	1.26	0.17
Cullin 1	7549752	100115.9	8.2	2	100.00	53.35	1.26	0.23
Hormone-sensitive lipase (Mus musculus domesticus)	677885	87018.7	6.5	2	100.00	60.78	1.25	0.03
Epoxide hydrolase 1	6753762	57724.5	8.4	2	100.00	53.93	1.24	0.10
Collagen, type VI, alpha 2 precursor	22203747	118822.8	6.0	11	100.00	63.77	1.24	0.16
Aldolase A, fructose-bisphosphate	42490830	43401.8	8.5	11	100.00	91.23	1.23	0.10
Preprocomplement component C3	309122	205041.7	6.4	6	100.00	56.08	1.23	0.18
Phosphatidylinositol-4-phosphate 5-kinase type II beta	17223780	50243.1	6.4	2	100.00	52.71	1.23	0.27
Fast skeletal myosin alkali light chain 1 isoform 1f	29789016	23699.5	5.0	14	100.00	97.84	1.22	0.18
Adenylate kinase 1	10946936	26311.9	5.7	5	100.00	77.64	1.22	0.24

Continued

Table 1. *Continued*

Protein name	Accession number	Protein MW	Protein PI	Peptide count	Total ion score, CI percentage	Best ion score	Average ratio (E4/E3)	Standard deviation (E4/E3)
Fibrinogen, alpha polypeptide, isoform CRA_b	148683477	68946.6	7.0	6	100.00	64.58	1.21	0.23
Lactate dehydrogenase A isoform 1	6754524	40772.0	7.6	13	100.00	74.65	1.21	0.13
Chain B, X-ray structure of the nucleosome core particle	27573730	12958.6	11.4	4	100.00	53.05	1.21	0.14
2′,3′-cyclic nucleotide 3′ phosphodiesterase isoform 2	226423907	53755.9	9.1	24	100.00	122.44	1.21	0.17
ATPase, H+ transporting, lysosomal V1 subunit H	14318722	60928.4	6.2	2	100.00	61.01	1.20	0.02
Chaperonin	460317	64225.7	8.2	2	100.00	98.95	1.20	0.15
Tyrosyl-tRNA synthetase	165377181	68152.2	6.6	2	100.00	40.36	1.20	0.14
Glyoxalase 1	19354350	23702.3	5.2	2	100.00	47.51	1.20	0.33
Xanthine dehydrogenase	187954915	159925.8	7.6	3	100.00	51.62	1.20	0.06

and outgrowth in many cell types, including neurons (41,50). More recently, however, it has become clear that regulated interactions between myosin and actin proteins in neurons are required for successful outgrowth and nerve regeneration. For example, many members of the myosin family of proteins are present in neuronal axons and synaptic terminals (42,51,52). Myosin proteins directly influence neurite outgrowth and retraction *in vitro* and *in vivo* (42,43), regulate the localization and distribution of cytoskeletal proteins in neurons (53–55) and also contribute to axonal pathfinding and neuronal development (56,57). In addition, similar to apoE, myosin 5A is synthesized locally following nerve injury (58), suggesting a role in delivering the required actin cytoskeleton for nerve regeneration *in vivo*. It is also likely that modified levels of myosin and actin proteins in non-neuronal cells would change the dynamics of the local microenvironment required for successful peripheral nerve regeneration. Thus, the widespread modification in expression levels of both myosin and actin proteins in apoE4 peripheral nerves may contribute to the impaired nerve regeneration observed in apoE4 mice. These initial insights suggest that more detailed biochemical investigations of the role of actin and myosin proteins in regulating apoE genotype-dependent regeneration of the peripheral nerve are now warranted.

Our proteomic experiments also revealed a significant influence of apoE genotype on the expression levels of proteins associated with haematological regulation, several of which are important for the integrity of the BBB/BNB. This finding was particularly interesting given that apoE has previously been shown to be essential for BBB and BNB integrity, although only in studies that examined the effect of complete loss of apoE, using apoE$^{-/-}$ mice (59,60). The data showing changes in levels of proteins including orosomucoid 1, fibrinogen, haptoglobin and haemopexin in uninjured and regenerating apoE4 nerves therefore provide insights into the potential molecular mechanisms through which apoE genotype can modulate haematological features associated with the nervous system. Orosomucoid 1, in particular, is a protein that modulates the permeability of the BBB (61), and was up-regulated in uninjured and regenerating nerves from apoE4 mice. Similarly, fibrinogen (up-regulated in apoE4 nerves) is a mediator of neuronal damage following disruption to the BBB (62). Although it is not possible at present to directly link the changes observed in haematological-related proteins to the deficient regeneration observed in apoE4 mice, the finding that disruption of the BNB impairs nerve regeneration (63) suggests that it may at least contribute to this response. Further work is now required to determine whether the specific proteins identified in the current study are also modified in the CNS, and whether they directly impair haematological regulation and BBB integrity in an apoE-genotype-dependent manner.

In summary, we have shown that apoE genotype is a significant determinant of the success of nerve regeneration in the PNS *in vivo*, with apoE4 selectively impairing regeneration of axons and re-innervation of NMJs following nerve injury in mice. Insights from comparative proteomic experiments demonstrated concomitant apoE-isoform-dependent changes in the peripheral nerve proteome, several of which are likely to have significant consequences for the form and function of the PNS.

MATERIALS AND METHODS

Mice

All animal experiments were approved by a University of Edinburgh internal ethics committee and were performed under license by the UK Home Office (project licence number 60/3891). Young adult mice expressing human apoE4 on a mouse apoE$^{-/-}$;C57BL/6J background were compared with littermate apoE$^{-/-}$ mice or apoE3 mice on an apoE$^{-/-}$;C57BL/6J background. For experiments examining the influence of loss of apoE, apoE$^{-/-}$ mice were compared with age-matched C57Bl/6J (WT) mice. Detailed information on the breeding and characteristics of apoE transgenic mice has previously been reported (35). Briefly, human apoE4 and apoE3 transgenic mice were generated on an apoE-deficient C57BL/6J background, utilizing human apoE4 or apoE3 transgenic constructs (35). Mice were supplied via a collaboration with Dr Allen Roses (Duke University) and breeding colonies established at the University of Edinburgh. ApoE4 and apoE3

Table 2. iTRAQ identification of proteins with >20% decreased expression and peptide count >1 in the unlesioned sciatic nerve from ApoE4 mice compared with ApoE3 mice

Protein name	Accession number	Protein MW	Protein PI	Peptide count	Total ion score, CI percentage	Best ion score	Average ratio (E4/E3)	Standard deviation (E4/E3)
Myosin, light polypeptide 6B	26986555	25852.8	5.4	4	100.00	69.41	0.19	0.12
Myoglobin	21359820	20131.1	7.1	10	100.00	143.49	0.49	0.07
Myosin, light polypeptide 3, isoform CRA_a	148677054	27359.4	5.0	5	100.00	54.09	0.51	1.25
h1-calponin alpha	1069994	36759.9	8.8	4	100.00	68.12	0.54	0.03
Igh protein	62028521	56919.8	7.5	3	100.00	71.06	0.57	0.08
Ig H-C allotype gamma2b	223428	40724.8	7.2	2	100.00	90.21	0.61	0.03
h-caldesmon	17017241	43428.3	5.3	2	100.00	70.01	0.63	0.25
Light chain of the monoclonal antibody MST2	1617395	27982.7	7.0	2	100.00	55.34	0.66	0.03
Skeletal muscle LIM protein	2880031	38678.1	8.8	2	100.00	78.07	0.67	0.02
Heat shock protein, alpha-crystallin-related, B6	59958370	18132.5	5.6	3	100.00	54.71	0.68	0.09
Chain A, crystal structure of mouse transthyretin	161172183	15211.9	5.8	3	100.00	94.87	0.69	0.08
Actinin alpha 2	157951643	112009.7	5.3	23	100.00	112.37	0.69	0.22
LIM domain binding 3 isoform b	84872213	76092.4	8.3	3	100.00	70.38	0.70	0.10
Filamin, alpha	125347376	305825.3	5.7	29	100.00	89.05	0.71	0.09
Fibromodulin precursor	10946680	44933.6	5.9	2	100.00	43.37	0.71	0.13
Milk fat globule-EGF factor 8 protein isoform 2	113865977	50796.5	6.7	5	100.00	83.22	0.71	0.08
Transgelin	6755714	25201.2	8.9	8	100.00	88.00	0.71	0.04
Myosin	1945080	253502.8	5.4	17	100.00	83.10	0.72	0.15
PDZ and LIM domain protein 3	7948997	36807.6	8.1	3	100.00	68.49	0.72	0.17
Myosin regulatory light polypeptide 9	198278553	22033.0	4.9	6	100.00	74.98	0.72	0.04
Collagen alpha-1(XIV) chain	146345398	206682.6	5.0	8	100.00	93.04	0.74	0.05
Procollagen, type I, alpha 2 precursor	111120329	136953.2	9.3	8	100.00	77.32	0.75	0.17
Destrin, isoform CRA_b	148696488	28666.5	9.0	5	100.00	66.15	0.76	0.08
LIM domain containing preferred translocation partner in lipoma isoform 1	225543157	71700.8	7.2	4	100.00	52.29	0.76	0.09
Actinin alpha 2	58476244	111806.5	5.3	20	100.00	112.37	0.76	0.27
Ig gamma-3 chain C region	121044	47963.7	6.7	3	100.00	46.58	0.76	0.03
Proteasome alpha 6 subunit	6755198	30608.7	6.3	3	100.00	75.58	0.77	0.21
Protein phosphatase 1	471976	42247.5	5.8	2	100.00	43.57	0.77	0.01
Chain A, crystal structure of the Ap-2 clathrin adaptor alpha	5822376	29953.4	6.9	2	100.00	49.31	0.78	0.06
Gfap protein	72679718	51278.8	5.1	3	100.00	45.03	0.78	0.19
Albumin precursor	163310765	77836.5	5.8	36	100.00	121.79	0.78	0.12
Probable ATP-dependent RNA helicase DDX5	2500527	74734.3	9.1	2	100.00	50.01	0.78	0.02
Adipsin precursor	7304867	29317.2	6.2	2	100.00	44.03	0.79	0.05
PDZ and LIM domain 5, isoform CRA_c	148680118	57492.2	8.2	3	100.00	82.11	0.79	0.09
Heterogeneous nuclear ribonucleoprotein L	183980004	68765.9	7.3	3	100.00	77.22	0.79	0.03
Fibulin 2	13529413	134192.5	4.6	2	100.00	43.20	0.79	0.02
EF hand domain containing 2	31981086	28253.9	5.0	2	100.00	43.24	0.79	0.17
Serpin peptidase inhibitor, clade C, member 1 precursor	18252782	57428.0	6.1	3	100.00	49.87	0.79	0.12
mKIAA0777 protein	28972395	139280.4	8.4	4	100.00	88.73	0.79	0.23
Carboxylesterase	192854	65222.7	5.0	8	100.00	84.01	0.80	0.11

transgenic mice were backcrossed with genetically homogeneous apoE-deficient mice (Charles River) for more than 10 generations (crossed to C57Bl/6J mice to reduce any genetic interference of the DBA/2 J background strain), resulting in mice heterozygous for the human apoE transgenes E4 or E3 on a homozygous mouse apoE background. The presence of mouse apoE genes was determined by PCR analysis of extracted DNA as described previously (35). Importantly, these mouse lines were selected for the current study, as apoE3 and apoE4 transgenes are known to be expressed at physiological levels, similar to those found in humans (9,35,64). All animals were housed in standard conditions and all procedures were carried out under licensed authority from the UK Home Office.

Surgery

Mice were anaesthetized by inhalation of halothane (2% in 1:1 N_2O/O_2) before exposing the sciatic nerve in the thigh or the tibial nerve above the heel. For nerve crush experiments, the sciatic or tibial nerve was crushed between a pair of fine-point forceps for 30 s. Nerves were checked to ensure a complete

Table 3. iTRAQ identification of proteins with >20% increased expression and peptide count >1 in regenerating sciatic nerve from ApoE4 mice compared with ApoE3 mice

Protein name	Accession number	Protein MW	Protein PI	Peptide count	Total ion score, CI percentage	Best ion score	Average ratio (E4/E3)	Standard deviation (E4/E3)
Haptoglobin precursor	8850219	42455.7	5.9	7	100.00	67.94	3.33	0.12
Orosomucoid 1	15215270	26393.8	5.4	5	100.00	58.65	1.90	0.15
PK-120 precursor	2739028	112522.4	6.1	2	100.00	52.16	1.87	0.01
Haemopexin precursor	160358829	55053.3	7.9	15	100.00	95.47	1.51	0.12
Calpain small subunit	19705421	24752.3	5.1	3	100.00	41.83	1.42	0.13
Unnamed protein product	26345578	19080.7	10.5	3	100.00	67.62	1.41	0.17
Laminin B1 subunit 1	114326497	221889.2	4.9	13	100.00	77.25	1.39	0.13
Fibrinogen, alpha polypeptide, isoform CRA_b	148683477	68946.6	7.0	6	100.00	64.58	1.38	0.09
Fibrinogen, gamma polypeptide	148683478	55480.4	5.4	6	100.00	84.66	1.38	0.09
CD10 neutral endopeptidase 24.11	192459	93776.9	5.7	2	100.00	52.20	1.37	0.23
Fibrinogen beta chain precursor	33859809	60169.0	6.7	12	100.00	78.56	1.35	0.12
C4 complement protein	50242	137077.1	6.5	2	100.00	47.28	1.34	0.13
2′,3′-cyclic nucleotide 3′ phosphodiesterase isoform 2	226423907	53755.9	9.1	24	100.00	122.44	1.33	0.13
Aspartyl-tRNA synthetase isoform 1	211065507	61980.2	6.1	2	100.00	63.91	1.33	0.03
Predicted: similar to major urinary protein 1	149252557	28801.5	5.1	4	100.00	85.86	1.32	0.08
Predicted: hypothetical protein isoform 2	82886943	18543.3	10.3	3	100.00	58.44	1.31	0.12
Hypoxanthine-guanine phosphoribosyltransferase	2499938	26555.9	5.7	3	100.00	48.91	1.30	0.08
Neural cell adhesion molecule 1 isoform 1	124517689	101275.8	4.8	3	100.00	46.03	1.29	0.13
Glutamine synthetase	31982332	45842.4	6.6	2	100.00	67.62	1.28	0.05
Nucleoside phosphorylase	7305395	34057.1	5.8	3	100.00	67.49	1.28	0.06
Auh protein	20072952	36020.8	9.6	2	100.00	56.44	1.27	0.04
Preprocomplement component C3	309122	205041.7	6.4	6	100.00	56.08	1.27	0.15
Microtubule-associated protein 6 isoform 1	113204613	107716.5	9.5	5	100.00	70.91	1.27	0.10
Nidogen 1 precursor	171543883	143072.8	5.2	23	100.00	76.48	1.27	0.10
Fbxo2 protein	20072543	34278.6	4.3	6	100.00	82.62	1.27	0.17
Laminin, alpha 2	117647249	376116.8	5.8	26	100.00	107.74	1.26	0.15
Breast carcinoma amplified sequence 1	123233481	58733.9	6.2	4	100.00	83.08	1.26	0.09
Solute carrier family 44, member 2	22779895	86584.2	9.1	2	100.00	66.29	1.25	0.15

crush had been performed before suturing the skin and allowing the mouse to recover. For nerve cut experiments, a ∼1 mm section of the nerve was removed to ensure complete transection. Post-operative mice were maintained in standard animal house conditions. The individual performing the surgery remained blind to the genotype of the mice, as were the individuals who performed all subsequent analyses, ensuring that operator bias could not adversely influence the experiments.

Electron microscopy

A 5 mm section of the peripheral nerve distal to the injury site was dissected out in 0.1 M EM-grade phosphate buffer and immediately fixed in 0.1 M phosphate buffer containing 4% paraformaldehyde/2.5% glutaraldehyde at 4°C. Nerves were post-fixed in 1% osmium tetroxide overnight. Following dehydration through an ascending series of ethanol solutions and propylene oxide, nerves were embedded in Durcupan resin. Ultrathin sections (∼60 nm) were cut and collected on formvar-coated grids (Agar Scientific, UK), stained with uranyl acetate and lead citrate and then quantitatively assessed in a Philips CM12 transmission electron microscope equipped with a Gatan camera. Using Adobe Photoshop, individual images were reconstructed to form entire nerve cross-sections. For regeneration experiments, higher power images were taken to allow assessment of large and small myelinated and unmyelinated axon profiles. All analysis was performed without the operator knowing the genetic status of the material.

Immunohistochemical analysis of NMJs

Mice were sacrificed by inhalation of isofluorane (2% in 1:1 N_2O/O_2). The levator auris longus (LAL; from the dorsal/ posterior surface of the neck) (65), transversus abdominis (from the anterolateral abdominal wall) (66), first to third deep lumbricals (from the plantar surface of the hind paw) (67) and/or flexor digitorum brevis (FDB; from the plantar surface of the hind paw) (67) muscles were dissected in oxygenated mammalian physiological saline (mM: NaCl 120, KCl 5, $CaCl_2$ 2, $MgCl_2$ 1, NaH_2PO_4 0.4, $NaHCO_3$ 23.8, D-glucose 5.6). Muscles were fixed in 0.1 M PBS containing 4% paraformaldehyde (Electron Microscopy Science) for 30 min. Muscles were exposed to α-bungarotoxin (α-BTX) conjugated to tetramethyl-rhodamine isocyanate (TRITC)-α-BTX; 5mg/ml, Molecular Probes) for 30 min to label post-synaptic

Table 4. iTRAQ identification of proteins with >20% decreased expression and peptide count >1 in regenerating sciatic nerve from ApoE4 mice compared with ApoE3 mice

Protein name	Accession number	Protein MW	Protein PI	Peptide count	Total ion score, CI percentage	Best ion score	Average ratio (E4/E3)	Standard deviation (E4/E3)
Myosin, light polypeptide 3, isoform CRA_a	148677054	27359.4	5.0	5	100.00	54.09	0.38	1.11
Troponin T	2340048	34082.0	9.4	4	100.00	78.26	0.39	0.50
Myozenin 1	10946924	34319.7	8.6	3	100.00	58.73	0.41	0.23
Myosin-binding protein C	81910387	143381.3	6.0	10	100.00	100.37	0.41	0.71
Myosin light chain, phosphorylatable, fast skeletal muscle	7949078	21485.1	4.8	11	100.00	99.81	0.42	0.94
Myomesin 2	170763465	179757.5	5.6	11	100.00	72.44	0.42	0.63
Calsequestrin 1	127798794	49034.3	3.9	3	100.00	83.23	0.43	0.28
Troponin C	6678371	19609.3	4.1	4	100.00	106.88	0.43	0.27
Fast skeletal myosin alkali light chain 1 isoform 1f	29789016	23699.5	5.0	14	100.00	97.84	0.43	0.82
Troponin I, skeletal, fast 2	123242973	25972.9	9.1	3	100.00	65.23	0.46	0.60
LIM domain binding 3 isoform f	84872217	33857.8	9.2	2	100.00	93.78	0.47	0.55
Muscle creatine kinase	6671762	48101.2	6.6	14	100.00	101.99	0.47	0.56
Myomesin 1 isoform 2	145279198	194032.5	6.0	7	100.00	81.84	0.48	0.54
Actinin alpha 3	7304855	110400.7	5.3	34	100.00	112.37	0.49	0.69
Nebulin	123857937	157734.8	8.8	2	100.00	45.87	0.51	0.63
Titin	123232572	3312853.3	6.2	2	100.00	37.84	0.53	0.25
Igh protein	62028521	56919.8	7.5	3	100.00	71.06	0.54	0.34
Alpha cardiac myosin heavy chain	191618	253883.5	5.6	18	100.00	91.72	0.55	0.25
Myh7 protein	187956918	252607.1	5.6	20	100.00	91.72	0.56	0.26
Myosin, heavy polypeptide 4, skeletal muscle	67189167	254149.5	5.6	86	100.00	127.38	0.56	0.38
LIM domain binding 3 isoform b	84872213	76092.4	8.3	3	100.00	70.38	0.56	0.10
Calcium/calmodulin-dependent protein kinase II alpha isoform 1	6753250	24580.7	6.5	1	99.85	50.17	0.56	0.02
Myosin, heavy polypeptide 8, skeletal muscle, perinatal	71143152	253848.8	5.7	46	100.00	106.43	0.56	0.41
Myosin heavy chain IIa	205830428	254268.0	5.6	58	100.00	123.29	0.56	0.38
Myosin, heavy polypeptide 8, skeletal muscle, perinatal	187956525	253835.8	5.7	47	100.00	106.43	0.57	0.40
Alpha-tropomyosin	157787199	38470.8	4.7	14	100.00	105.62	0.58	0.35
Myosin, heavy polypeptide 1, skeletal muscle, adult	82524274	254200.7	5.6	71	100.00	127.38	0.58	0.38
Ig H-C allotype gamma2b	223428	40724.8	7.2	2	100.00	90.21	0.59	0.26
Sarcalumenin, isoform CRA_a	148664814	59761.7	6.2	4	100.00	60.15	0.60	0.36
mCG18455	148678485	256334.6	5.5	22	100.00	84.80	0.60	0.39
Tropomyosin 1, alpha, isoform CRA_b	148694194	37823.3	4.7	12	100.00	105.62	0.60	0.39
Predicted: similar to tropomyosin 2 (beta) isoform 2 isoform 15	73971296	38348.4	4.6	17	100.00	86.54	0.61	0.30
Adenylate kinase 1	10946936	26311.9	5.7	5	100.00	77.64	0.63	0.25
Tropomyosin 1, alpha isoform i	78000203	32304.2	4.7	11	100.00	105.62	0.63	0.44
Muscle glycogen phosphorylase	6755256	104509.5	6.7	18	100.00	93.56	0.63	0.32
Myoglobin	21359820	20131.1	7.1	10	100.00	143.49	0.64	0.43
RIKEN cDNA 8030451F13, isoform CRA_c	148689541	142202.0	5.7	4	100.00	52.26	0.64	0.50
Enolase 3, beta muscle, isoform CRA_a	148680653	54402.9	6.8	15	100.00	112.63	0.64	0.60
Actin, alpha 1, skeletal muscle	4501881	45181.8	5.2	12	100.00	91.76	0.65	0.46
mCG2006, isoform CRA_a	148680420	187536.8	6.3	2	100.00	60.73	0.65	0.06
Actinin alpha 2	58476244	111806.5	5.3	20	100.00	112.37	0.65	0.39
ATPase, Ca^{++} transporting, ubiquitous isoform a	254039658	116671.4	5.5	2	100.00	48.16	0.66	0.09
Alpha actin 1 proprotein	4885049	45033.8	5.2	12	100.00	91.76	0.66	0.45
Alpha 2 actin	4501883	45185.8	5.2	12	100.00	91.76	0.66	0.48
Methylthioadenosine phosphorylase, isoform CRA_b	148699009	36228.5	6.5	2	100.00	43.65	0.67	0.19
Actinin alpha 2	157951643	112009.7	5.3	23	100.00	112.37	0.67	0.34
Myosin	1945080	253502.8	5.4	17	100.00	83.10	0.67	0.39
Heat shock protein, alpha-crystallin-related, B6	59958370	18132.5	5.6	3	100.00	54.71	0.67	0.17
Sarcomeric mitochondrial creatine kinase precursor	38259206	51557.9	8.6	2	100.00	46.62	0.69	0.37
Adenylosuccinate synthase like 1	6671519	54920.1	8.6	2	100.00	81.76	0.69	0.07
Growth factor receptor bound protein 2	6680083	27765.1	5.7	2	100.00	45.66	0.69	0.41
ATPase, Ca^{++} transporting, cardiac muscle, fast twitch 1	148685412	116243.4	5.3	12	100.00	114.25	0.70	0.14
PDZ and LIM domain protein 3	7948997	36807.6	8.1	3	100.00	68.49	0.70	0.13
mCG147612, isoform CRA_b	148686595	58853.2	5.8	4	100.00	49.09	0.70	0.24
h1-calponin alpha	1069994	36759.9	8.8	4	100.00	68.12	0.72	0.23

Continued

Table 4. *Continued*

Protein name	Accession number	Protein MW	Protein PI	Peptide count	Total ion score, CI percentage	Best ion score	Average ratio (E4/E3)	Standard deviation (E4/E3)
Myosin, light polypeptide kinase	55930915	237267.2	6.0	2	100.00	46.40	0.72	0.24
Parvalbumin	31980767	14372.8	5.0	5	100.00	88.79	0.72	0.41
UDP-glucose ceramide glucosyltransferase-like 1	45946485	190971.6	5.4	2	100.00	43.57	0.72	0.02
Predicted: similar to tropomyosin 3 isoform 1	149751320	32645.1	4.8	10	100.00	80.10	0.74	0.37
Carboxylesterase	192854	65222.7	5.0	8	100.00	84.01	0.74	0.09
Phosphoglycerate mutase 2	9256624	31972.9	8.7	8	100.00	89.17	0.74	0.54
Skeletal muscle LIM protein	2880031	38678.1	8.8	2	100.00	78.07	0.75	0.23
RIKEN cDNA 1810020D17, isoform CRA_c	148684357	17880.5	7.8	2	100.00	44.25	0.75	0.09
Aldolase A, fructose-bisphosphate	42490830	43401.8	8.5	11	100.00	91.23	0.75	0.17
Albumin precursor	163310765	77836.5	5.8	36	100.00	121.79	0.77	0.26
SH3P9	1438563	53597.8	5.1	4	100.00	62.83	0.77	0.12
Creatine kinase, mitochondrial 1, ubiquitous, isoform CRA_c	148696104	50564.3	8.5	2	100.00	59.05	0.77	0.04
Milk fat globule-EGF factor 8 protein isoform 2	113865977	50796.5	6.7	5	100.00	83.22	0.77	0.20
ATPase, Ca^{++} transporting, slow twitch 2 isoform a	158635979	124907.5	5.2	5	100.00	68.51	0.78	0.32
Proteasome alpha 6 subunit	6755198	30608.7	6.3	2	100.00	75.58	0.78	0.18
Liver glycogen phosphorylase	18875342	107417.7	6.6	5	100.00	58.28	0.78	0.28
Solute carrier family 4 (anion exchanger), member 1	6755560	108215.2	5.4	2	100.00	50.97	0.78	0.06
Coagulation factor II	123227411	76215.8	6.0	4	100.00	61.55	0.79	0.08
TRIO and F-actin binding protein isoform 3	88501749	234306.2	8.4	2	100.00	36.79	0.79	0.04
Ig gamma-3 chain C region	121044	47963.7	6.7	3	100.00	46.58	0.79	0.01
Filamin, alpha	125347376	305825.3	5.7	29	100.00	89.05	0.79	0.20
Glyceraldehyde-3-phosphate-dehydrogenase isoform 1	149272161	40122.8	7.1	3	100.00	86.97	0.79	0.05
Phosphoglucomutase 2	55824767	66748.2	6.0	10	100.00	75.31	0.80	0.23
C-1-tetrahydrofolate synthase, cytoplasmic	34921990	110015.8	6.9	2	100.00	40.34	0.80	0.31
Alpha actinin 1a	82659196	111086.8	5.3	32	100.00	112.37	0.80	0.33
Acyl-CoA thioesterase 2	39992610	52675.7	7.2	2	100.00	53.32	0.80	0.22

acetylcholine receptors. Muscles were then immunohistochemically processed to allow visualization of pre-synaptic motor nerve terminals, as described previously (68). Briefly, muscles were blocked in 4% bovine serum albumin and 1.5% Triton X-100 in 0.1 M PBS for 30 min before incubation in primary antibodies directed against 145 kDa neurofilament proteins (1:250 dilution; Millipore) overnight. After washing for 2 h in 0.1 M PBS, muscles were incubated for 4 h in a 1:30 dilution of swine anti-rabbit secondary antibody conjugated to the fluorescent label FITC (Dako). Muscles were then whole-mounted in Mowoil® (Calbiochem) on glass slides and cover-slipped for subsequent imaging.

Microscopy

Fluorescently labelled muscle preparations were viewed using either a standard epi-fluorescence microscope equipped with a chilled CCD camera (40× objective; 0.8 NA; Nikon IX71 microscope; Hammamatsu C4742–95) or a laser scanning confocal microscope (63× objective; 1.4 NA; Zeiss LSM710). TRITC-α-BTX-labelled preparations were imaged using 543 nm excitation and 590 nm emission optics, and FITC-labelled preparations utilized 488 nm excitation and 520 nm emission optics. For confocal microscopy, 488 and 543 nm laser lines were used for excitation, and confocal Z-series were merged using ImageJ software. All images were then assembled for analysis, using Adobe Photoshop. A minimum of 80 NMJs, selected at random, were assessed in each muscle preparation. Muscles where antibody staining was too faint to quantify due to poor antibody penetration and muscles with damage to either the muscle fibres or nerves from dissection were excluded from further analysis. All analyses were performed without the operator knowing the genetic status of the material. For occupancy counts, endplates were categorized as either vacant (no neurofilament overlying the endplate), partially occupied (neurofilament partially overlying the endplate) or fully occupied (neurofilament entirely overlying the endplate). For the assessment of developmental synapse elimination, fully occupied endplates were further subdivided on the basis of the number of axonal inputs contacting the endplate. For neuromuscular re-innervation experiments, an individual endplate was required to be fully occupied by an incoming single axon profile to be considered re-innervated.

Electrophysiology

Freshly dissected FDB muscles were used to obtain intracellular recordings (69) of evoked EPPs and spontaneous mEPPs. Isolated muscles were pinned out in a Sylgard (VWR International, Poole, UK)-lined bath and perfused with oxygenated mammalian physiological saline (see above). Muscle contractions were reduced or eliminated by bathing the muscles in 2.5 μM μ-conotoxin GIIIB (Scientific Marketing Associates,

UK) for 30–45 min. Thirty muscle fibres per muscle were sampled using glass microelectrodes filled with 4 M potassium acetate (impedance ~30–40 MΩ), according to standard techniques. Spontaneous and evoked EPPs were recorded using Axoclamp 2B amplifiers (Axon Instruments) and stored and analysed on a PC using WinWCP v3.9.5 software (developed and distributed by Dr John Dempster, Strathclyde University). Average frequency of spontaneous MEPPs was obtained from continuous records of 10–60 s duration. The quantal content of EPPs was determined from measurements of peak EPP amplitude in trains evoked at stimulation frequencies of 0.5–2 Hz, using the variance method and applying the McLachlan–Martin formula for correction of non-linear summation of EPPs (70), with the modifier $f = 3D0.3$.

iTRAQ proteomics

Unlesioned tibial nerves from nine apoE3 and nine apoE4 mice were pooled into three groups for each genotype, and underwent iTRAQ proteomic analysis. This was repeated with nine nerves from each genotype 3 weeks after tibial nerve crush. Nerves were extracted in buffer containing 6 M urea, 2 M thiourea, 2% CHAPS and 0.5% SDS in dH_2O. The proteins were precipitated in six volumes of ice-cold acetone overnight at −20°C. Acetone precipitates were pelleted by centrifugation at 13 000*g* for 10 min at 4°C and the supernatant was carefully removed and discarded. The pellets were allowed to air-dry, followed by resuspension in 6 M urea in 50 mM TEAB. The protein concentration in each group was determined using a Bradford assay.

Reduction, alkylation and digestion steps were performed using the reagents and according to the recommendations in the iTRAQ labelling kit (Applied Biosystems). The extracts were diluted with 50 mM TEAB so that the urea concentration was <1 M, before the addition of trypsin and overnight incubation at 37°C. The digests were then dried down in a vacuum centrifuge and iTRAQ labelling was carried out according to the instructions in the iTRAQ labelling kit. The iTRAQ tags were assigned to samples as follows: 115-ApoE3 and 117-ApoE4. Each tag was incubated with 85 μg of protein (as determined by a Bradford protein assay).

iTRAQ-labelled peptides were pooled and made up to a total volume of 2.4 ml in strong cation-exchange (SCX) buffer A [10 mM phosphate, pH 3, in 20% acetonitrile (Romil, UK)]. The pooled peptides (2.4 ml) were then separated by SCX chromatography using a polysulfoethyl A column, 300 Å, 5 μM (PolyLC)) at a flow rate of 400 μl/min. Following sample injection, the column was washed with SCX buffer A until the baseline returned. The gradient was run as follows: 0–50% SCX buffer B (10 mM phosphate, 1 M NaCl, pH3, in 20% acetonitrile) over 25 min followed by a ramp up from 50 to 100% SCX buffer B over 5 min. The column was then washed in 100% SCX buffer B for 5 min before equilibrating for 10 min with SCX buffer A. Fractions were collected (400 μl) during the elution period and dried down completely in a vacuum centrifuge.

The iTRAQ tryptic peptide fractions were each resuspended in 30 μl of RP buffer A (2% acetonitrile, 0.05% TFA in water; Sigma Chromasolv plus). Prior to mass spectrometry analysis, fractions were first separated by liquid chromatography (Dionex Ultimate 3000) on a Pepmap C18 column, 200 μm × 15 cm (LC Packings) at a flow rate of 3 μl/min. Fractions were injected by full-loop injection (20 μl) and the order of loading was randomized to minimize effects from carryover. The eluants used were (A) 0.05% TFA in 2% acetonitrile in water and (B) 0.05% TFA in 90% acetonitrile in water. The gradient was run as follows: 10 min isocratic pre-run at 100% A, followed by a linear gradient from 0 to 30% B over 100 min, followed by another linear gradient from 30 to 60% over 35 min. The column was then washed in 100% B for a further 10 min, before a final equilibration step in 100% A for 10 min. During the elution gradient, the sample was spotted at 10 s intervals using a Probot (LC Packings) with α-cyano-4-hydroxycinnamic acid at 3 mg/ml (70% MeCN, 0.1% TFA) at a flow rate of 1.2 μl/min.

Both MS and MS/MS analyses were performed on the fractionated peptides using an Applied Biosystems 4800 MALDI TOF/TOF mass spectrometer. The mass spectrometer was operated under the control of 4000 Series Explorer v3.5.2 software (Applied Biosystems). A total of 1000 shots per MS spectrum (no-stop conditions) and 2500 shots per MS/MS spectrum (no-stop conditions) were acquired. The following MS/MS acquisition settings were used: 2 kV operating mode with CID on and precursor mass window resolution set to 300.00 (FWHM). Peak lists of MS and MS/MS spectra were generated using 4000 Series Explorer v3.5.2 software and the following parameters were used after selective labelling of monoisotopic mass peaks: MS peak lists: S/N threshold 10, Savitzky Golay smoothing [three points across peak (FWHM)], no baseline correction; MS/MS peak lists: S/N threshold 14, Savitzky Golay smoothing [seven points across peak (FWHM)].

An automated database search was run using GPS Explorer v3.6 (Applied Biosystems). MASCOT was used as the search engine to search the NCBI non-redundant database (version 10/11/2009), using the following search parameters: precursor ion mass tolerance of 100 p.p.m., MS/MS fragment ion mass tolerance of 0.3 Da and iTRAQ fragment ion mass tolerance of 0.2 Da. The enzyme was specified as trypsin with one missed cleavage permitted, oxidation of methionine residues were allowed as variable modifications and N-terminal (iTRAQ), lysine (iTRAQ) and MMTS modification of cysteine residues were set as fixed modifications and the taxonomy was selected as Mus. The identification criterion was at least two unique peptides by MS/MS with the most stringent search settings in order to yield the most reliable data for iTRAQ quantification (peptide rank 1 and total ion score confidence intervals of at least 95%).

Peptides were reported as identified iTRAQ peptides only if they met the following criteria: iTRAQ ratio of greater than 0, all N-terminal and lysine residues were labelled and did not include tyrosine_iTRAQ modification. Quantification of the iTRAQ peptides was performed by applying the following formula: corrected cluster area of fragment/corrected cluster area of reference [i.e. 117 (ApoE4)/115 (ApoE3)]. Following correction using kit-specific iTRAQ correction factors, iTRAQ ratios were normalized to the median ratio, using the following formula: iTRAQ ratio = ratio/median iTRAQ ratio of all found pairs. Both correction and normalization were performed using GPS Explorer software v3.6.

To obtain further insights into cellular pathways and protein interaction networks modified as a result of apoE genotype, the IPA application (Ingenuity Systems) was used. IPA dynamically generates network of gene, protein, small molecule, drug and disease associations on the basis of 'hand-curated' data held in a proprietary database. Changes in specific protein interaction networks were identified on the basis of the number and percentage of candidate proteins contributing to the entire network.

Quantitative fluorescent (Li-COR) western blots

Total protein was isolated from distal nerve stumps and quantitative western blots were performed as described previously (71–73). Briefly, protein was separated by SDS/polyacrylamide gel electrophoresis on 4–20% pre-cast NuPage 4–12% Bis Tris gradient gels (Invitrogen) and then transferred to PVDF membrane overnight. The membranes were blocked using Odyssey blocking buffer (Li-COR) and incubated with primary antibodies as per manufacturers' instructions (apoE, Millipore; tubulin, Abcam). Odyssey secondary antibodies were added according to manufacturer's instructions (donkey anti-goat IRDye 680 and goat anti-rabbit IRDye 680). Blots were imaged using an Odyssey Infrared Imaging System (Li-COR Biosciences).

Statistical analysis

All data were collected into Microsoft Excel spreadsheets and analysed using GraphPad Prism software. All bar charts shown are mean $\pm$ SEM. Statistical significance was considered to be $P < 0.05$ for all analyses. Individual statistical tests used are detailed in figure legends.

SUPPLEMENTARY MATERIAL

Supplementary Material is available at *HMG* online.

ACKNOWLEDGEMENTS

The provision of the apoE transgenic mice via a collaboration with Dr Allen Roses is gratefully acknowledged.

Conflict of Interest statement. None declared.

FUNDING

This work was supported by research grants from the Biotechnology and Biological Sciences Research Council (to T.H.G./L.H.C.); Anatomical Society of Great Britain and Ireland (to T.H.G./S.H.P.); Medical Research Scotland (to T.H.G.); Help the Aged/Age Concern (to K.H.); and the Wellcome Trust (to K.H./T.H.G.).

REFERENCES

1. Horsburgh, K., McCarron, M.O., White, F. and Nicoll, J.A. (2000) The role of apolipoprotein E in Alzheimer's disease, acute brain injury and cerebrovascular disease: evidence of common mechanisms and utility of animal models. *Neurobiol. Aging*, **21**, 245–255.
2. Mahley, R.W., Huang, Y. and Weisgraber, K.H. (2006) Putting cholesterol in its place: apoE and reverse cholesterol transport. *J. Clin. Invest.*, **116**, 1226–1229.
3. Corder, E.H., Saunders, A.M., Strittmatter, W.J., Schmechel, D.E., Gaskell, P.C., Small, G.W., Roses, A.D., Haines, J.L. and Pericak-Vance, M.A. (1993) Gene dose of apolipoprotein E type 4 allele and the risk of Alzheimer's disease in late onset families. *Science*, **261**, 921–923.
4. Saunders, A.M., Schmader, K., Breitner, J.C., Benson, M.D., Brown, W.T., Goldfarb, L., Goldgaber, D., Manwaring, M.G., Szymanski, M.H., McCown, N. *et al.* (1993) Apolipoprotein E epsilon 4 allele distributions in late-onset Alzheimer's disease and in other amyloid-forming diseases. *Lancet*, **342**, 710–711.
5. Saunders, A.M., Strittmatter, W.J., Schmechel, D., George-Hyslop, P.H., Pericak-Vance, M.A., Joo, S.H., Rosi, B.L., Gusella, J.F., Crapper-MacLachlan, D.R., Alberts, M.J. *et al.* (1993) Association of apolipoprotein E allele epsilon 4 with late-onset familial and sporadic Alzheimer's disease. *Neurology*, **43**, 1467–1472.
6. Li, Y.J., Hauser, M.A., Scott, W.K., Martin, E.R., Booze, M.W., Qin, X.J., Walter, J.W., Nance, M.A., Hubble, J.P., Koller, W.C. *et al.* (2004) Apolipoprotein E controls the risk and age at onset of Parkinson disease. *Neurology*, **62**, 2005–2009.
7. Zareparsi, S., Kaye, J., Camicioli, R., Grimslid, H., Oken, B., Litt, M., Nutt, J., Bird, T., Schellenberg, G. and Payami, H. (1997) Modulation of the age at onset of Parkinson's disease by apolipoprotein E genotypes. *Ann. Neurol.*, **42**, 655–658.
8. Alberts, M.J., Graffagnino, C., McClenny, C., DeLong, D., Strittmatter, W., Saunders, A.M. and Roses, A.D. (1995) ApoE genotype and survival from intracerebral haemorrhage. *Lancet*, **346**, 575.
9. Horsburgh, K., McCulloch, J., Nilsen, M., Roses, A.D. and Nicoll, J.A. (2000) Increased neuronal damage and apoE immunoreactivity in human apolipoprotein E, E4 isoform-specific, transgenic mice after global cerebral ischaemia. *Eur. J. Neurosci.*, **12**, 4309–4317.
10. McColl, B.W., McGregor, A.L., Wong, A., Harris, J.D., Amalfitano, A., Magnoni, S., Baker, A.H., Dickson, G. and Horsburgh, K. (2007) APOE epsilon3 gene transfer attenuates brain damage after experimental stroke. *J. Cereb. Blood Flow Metab.*, **27**, 477–487.
11. Teasdale, G.M., Murray, G.D. and Nicoll, J.A. (2005) The association between APOE epsilon4, age and outcome after head injury: a prospective cohort study. *Brain*, **128**, 2556–2561.
12. Teasdale, G.M., Nicoll, J.A., Murray, G. and Fiddes, M. (1997) Association of apolipoprotein E polymorphism with outcome after head injury. *Lancet*, **350**, 1069–1071.
13. Schiefermeier, M., Kollegger, H., Madl, C., Polli, C., Oder, W., Kühn, H., Berr, F. and Ferenci, P. (2000) The impact of apolipoprotein E genotypes on age at onset of symptoms and phenotypic expression in Wilson's disease. *Brain*, **123**, 585–590.
14. Bedlack, R.S., Strittmatter, W.J. and Morgenlander, J.C. (2000) Apolipoprotein E and neuromuscular disease: a critical review of the literature. *Arch. Neurol.*, **57**, 1561–1565.
15. Geranmayeh, F., Christian, L., Turkheimer, F.E., Gentleman, S.M. and O'Neill, K.S. (2005) A need to clarify the role of apolipoprotein E in peripheral nerve injury and repair. *J. Peripher. Nerv. Syst.*, **10**, 344–345.
16. Akaaboune, M., Villanova, M., Festoff, B.W., Verdiere-Sahuque, M. and Hantai, D. (1994) Apolipoprotein E expression at neuromuscular junctions in mouse, rat and human skeletal muscle. *FEBS Lett.*, **351**, 246–248.
17. Boyles, J.K., Pitas, R.E., Wilson, E., Mahley, R.W. and Taylor, J.M. (1985) Apolipoprotein E associated with astrocytic glia of the central nervous system and with nonmyelinating glia of the peripheral nervous system. *J. Clin. Invest.*, **76**, 1501–1513.
18. Gelman, B.B., Rifai, N., Goodrum, J.F., Bouldin, T.W. and Krigman, M.R. (1987) Apolipoprotein E is released by rat sciatic nerve during segmental demyelination and remyelination. *J. Neuropathol. Exp. Neurol.*, **46**, 644–652.
19. Ignatius, M.J., Gebicke-Harter, P.J., Skene, J.H., Schilling, J.W., Weisgraber, K.H., Mahley, R.W. and Shooter, E.M. (1986) Expression of apolipoprotein E during nerve degeneration and regeneration. *Proc. Natl Acad. Sci. USA*, **83**, 1125–1129.
20. Skene, J.H. and Shooter, E.M. (1983) Denervated sheath cells secrete a new protein after nerve injury. *Proc. Natl Acad. Sci. USA*, **80**, 4169–4173.
21. Bedlack, R.S., Edelman, D., Gibbs, J.W. III, Kelling, D., Strittmatter, W., Saunders, A.M. and Morgenlander, J. (2003) APOE genotype is a risk factor for neuropathy severity in diabetic patients. *Neurology*, **60**, 1022–1024.

22. Tsuzuki, S., Murano, T., Watanabe, H., Itoh, Y., Miyashita, Y. and Shirai, K. (1998) The examination of apoE phenotypes in diabetic patients with peripheral neuropathy. *Rinsho Byori*, **46**, 829–833.
23. al-Chalabi, A., Enayat, Z.E., Bakker, M.C., Sham, P.C., Ball, D.M., Shaw, C.E., Lloyd, C.M., Powell, J.F. and Leigh, P.N. (1996) Association of apolipoprotein E epsilon 4 allele with bulbar-onset motor neuron disease. *Lancet*, **347**, 159–160.
24. Bachus, R., Bader, S., Gessner, R. and Ludolph, A.C. (1997) Lack of association of apolipoprotein E epsilon 4 allele with bulbar-onset motor neuron disease. *Ann. Neurol.*, **41**, 417.
25. Drory, V.E. and Artmonov, I. (2007) Earlier onset and shorter survival of amyotrophic lateral sclerosis in Jewish patients of North African origin. A clue to modifying genetic factors? *J. Neurol. Sci.,* **258**, 39–43.
26. Drory, V.E., Birnbaum, M., Korczyn, A.D. and Chapman, J. (2001) Association of APOE epsilon4 allele with survival in amyotrophic lateral sclerosis. *J. Neurol. Sci.*, **190**, 17–20.
27. Li, Y.J., Pericak-Vance, M.A., Haines, J.L., Siddique, N., McKenna-Yasek, D., Hung, W.Y., Sapp, P., Allen, C.I., Chen, W., Hosler, B. *et al.* (2004) Apolipoprotein E is associated with age at onset of amyotrophic lateral sclerosis. *Neurogenetics*, **5**, 209–213.
28. Moulard, B., Sefiani, A., Laamri, A., Malafosse, A. and Camu, W. (1996) Apolipoprotein E genotyping in sporadic amyotrophic lateral sclerosis: evidence for a major influence on the clinical presentation and prognosis. *J. Neurol. Sci.*, **139**, 34–37.
29. Mui, S., Rebeck, G.W., McKenna-Yasek, D., Hyman, B.T. and Brown, R.H. Jr (1995) Apolipoprotein E epsilon 4 allele is not associated with earlier age at onset in amyotrophic lateral sclerosis. *Ann. Neurol.*, **38**, 460–463.
30. Olsen, M.K., Roberds, S.L., Ellerbrock, B.R., Fleck, T.J., McKinley, D.K. and Gurney, M.E. (2001) Disease mechanisms revealed by transcription profiling in SOD1-G93A transgenic mouse spinal cord. *Ann. Neurol.*, **50**, 730–740.
31. Siddique, T., Pericak-Vance, M.A., Caliendo, J., Hong, S.T., Hung, W.Y., Kaplan, J., McKenna-Yasek, D., Rimmler, J.B., Sapp, P., Saunders, A.M. *et al.* (1998) Lack of association between apolipoprotein E genotype and sporadic amyotrophic lateral sclerosis. *Neurogenetics*, **1**, 213–216.
32. Smith, R.G., Haverkamp, L.J., Case, S., Appel, V. and Appel, S.H. (1996) Apolipoprotein E epsilon 4 in bulbar-onset motor neuron disease. *Lancet*, **348**, 334–335.
33. Genden, E.M., Watanabe, O., Mackinnon, S.E., Hunter, D.A. and Strasberg, S.R. (2002) Peripheral nerve regeneration in the apolipoprotein-E-deficient mouse. *J. Reconstr. Microsurg.*, **18**, 495–502.
34. Popko, B., Goodrum, J.F., Bouldin, T.W., Zhang, S.H. and Maeda, N. (1993) Nerve regeneration occurs in the absence of apolipoprotein E in mice. *J. Neurochem.*, **60**, 1155–1158.
35. Xu, P.T., Schmechel, D., Rothrock-Christian, T., Burkhart, D.S., Qiu, H.L., Popko, B., Sullivan, P., Maeda, N., Saunders, A.M., Roses, A.D. *et al.* (1996) Human apolipoprotein E2, E3, and E4 isoform-specific transgenic mice: human-like pattern of glial and neuronal immunoreactivity in central nervous system not observed in wild-type mice. *Neurobiol. Dis.*, **3**, 229–245.
36. Belinson, H., Lev, D., Masliah, E. and Michaelson, D.M. (2008) Activation of the amyloid cascade in apolipoprotein E4 transgenic mice induces lysosomal activation and neurodegeneration resulting in marked cognitive deficits. *J. Neurosci.*, **28**, 4690–4701.
37. Malek, G., Johnson, L.V., Mace, B.E., Saloupis, P., Schmechel, D.E., Rickman, D.W., Toth, C.A., Sullivan, P.M. and Bowes Rickman, C. (2005) Apolipoprotein E allele-dependent pathogenesis: a model for age-related retinal degeneration. *Proc. Natl Acad. Sci. USA*, **102**, 11900–11905.
38. Tesseur, I., Van Dorpe, J., Bruynseels, K., Bronfman, F., Sciot, R., Van Lommel, A. and Van Leuven, F. (2000) Prominent axonopathy and disruption of axonal transport in transgenic mice expressing human apolipoprotein E4 in neurons of brain and spinal cord. *Am. J. Pathol.*, **157**, 1495–1510.
39. Miledi, R. and Slater, C.R. (1970) On the degeneration of rat neuromuscular junctions after nerve section. *J. Physiol.*, **207**, 507–528.
40. Gillingwater, T.H. and Ribchester, R.R. (2001) Compartmental neurodegeneration and synaptic plasticity in the Wld(s) mutant mouse. *J. Physiol.*, **534**, 627–639.
41. Arnold, D.B. (2009) Actin and microtubule-based cytoskeletal cues direct polarized targeting of proteins in neurons. *Sci. Signal.*, **2**, 49.
42. Brown, M.E. and Bridgman, P.C. (2004) Myosin function in nervous and sensory systems. *J. Neurobiol.*, **58**, 118–130.
43. Chantler, P.D. and Wylie, S.R. (2003) Elucidation of the separate roles of myosins IIA and IIB during neurite outgrowth, adhesion and retraction. *IEE Proc. Nanobiotechnol.*, **150**, 111–125.
44. Bellosta, S., Nathan, B.P., Orth, M., Dong, L.M., Mahley, R.W. and Pitas, R.E. (1995) Stable expression and secretion of apolipoproteins E3 and E4 in mouse neuroblastoma cells produces differential effects on neurite outgrowth. *J. Biol. Chem.*, **270**, 27063–27071.
45. Nathan, B.P., Bellosta, S., Sanan, D.A., Weisgraber, K.H., Mahley, R.W. and Pitas, R.E. (1994) Differential effects of apolipoproteins E3 and E4 on neuronal growth *in vitro*. *Science*, **264**, 850–852.
46. Teter, B., Xu, P.T., Gilbert, J.R., Roses, A.D., Galasko, D. and Cole, G.M. (2002) Defective neuronal sprouting by human apolipoprotein E4 is a gain-of-negative function. *J. Neurosci. Res.*, **68**, 331–336.
47. White, F., Nicoll, J.A., Roses, A.D. and Horsburgh, K. (2001) Impaired neuronal plasticity in transgenic mice expressing human apolipoprotein E4 compared to E3 in a model of entorhinal cortex lesion. *Neurobiol. Dis.*, **8**, 611–625.
48. Corder, E.H., Robertson, K., Lannfelt, L., Bogdanovic, N., Eggertsen, G., Wilkins, J. and Hall, C. (1998) HIV-infected subjects with the E4 allele for APOE have excess dementia and peripheral neuropathy. *Nat. Med.*, **4**, 1182–1184.
49. Schaefer, A.M., Sanes, J.R. and Lichtman, J.W. (2005) A compensatory subpopulation of motor neurons in a mouse model of amyotrophic lateral sclerosis. *J. Comp. Neurol.*, **490**, 209–219.
50. McQuarrie, I.G. and Lund, L.M. (2009) Intra-axonal myosin and actin in nerve regeneration. *Neurosurgery*, **65**, A93–A96.
51. Bearer, E.L., DeGiorgis, J.A., Bodner, R.A., Kao, A.W. and Reese, T.S. (1993) Evidence for myosin motors on organelles in squid axoplasm. *Proc. Natl Acad. Sci. USA*, **90**, 11252–11256.
52. Vega-Riveroll, L.J., Wylie, S.R., Loughna, P.T., Parson, S.H. and Chantler, P.D. (2005) Nonmuscle myosins IIA and IIB are present in adult motor nerve terminals. *Neuroreport*, **16**, 1143–1146.
53. Rao, M.V., Engle, L.J., Mohan, P.S., Yuan, A., Qiu, D., Cataldo, A., Hassinger, L., Jacobsen, S., Lee, V.M., Andreadis, A. *et al.* (2002) Myosin Va binding to neurofilaments is essential for correct myosin Va distribution and transport and neurofilament density. *J. Cell Biol.*, **159**, 279–290.
54. Schaefer, A.W., Schoonderwoert, V.T., Ji, L., Mederios, N., Danuser, G. and Forscher, P. (2008) Coordination of actin filament and microtubule dynamics during neurite outgrowth. *Dev. Cell*, **15**, 146–162.
55. Alami, N.H., Jung, P. and Brown, A. (2009) Myosin Va increases the efficiency of neurofilament transport by decreasing the duration of long-term pauses. *J. Neurosci.*, **29**, 6625–6634.
56. Zhu, X.J., Wang, C.Z., Dai, P.G., Xie, Y., Song, N.N., Liu, Y., Du, Q.S., Mei, L., Ding, Y.Q. and Xiong, W.C. (2007) Myosin X regulates netrin receptors and functions in axonal path-finding. *Nat. Cell Biol.*, **9**, 184–192.
57. Ma, X., Kawamoto, S., Uribe, J. and Adelstein, R.S. (2006) Function of the neuron-specific alternatively spliced isoforms of nonmuscle myosin II-B during mouse brain development. *Mol. Biol. Cell*, **17**, 2138–2149.
58. Calliari, A., Sotelo-Silveira, J., Costa, M.C., Nogueira, J., Cameron, L.C., Kun, A., Benech, J. and Sotelo, J.R. (2002) Myosin Va is locally synthesized following nerve injury. *Cell Motil. Cytoskeleton*, **51**, 169–176.
59. Fullerton, S.M., Shirman, G.A., Strittmatter, W.J. and Matthew, W.D. (2001) Impairment of the blood–nerve and blood–brain barriers in apolipoprotein e knockout mice. *Exp. Neurol.*, **169**, 13–22.
60. Methia, N., André, P., Hafezi-Moghadam, A., Economopoulos, M., Thomas, K.L. and Wagner, D.D. (2001) ApoE deficiency compromises the blood brain barrier especially after injury. *Mol. Med.*, **7**, 810–815.
61. Yuan, W., Li, G., Zeng, M. and Fu, B.M. (2010) Modulation of the blood–brain barrier permeability by plasma glycoprotein orosomucoid. *Microvasc. Res.*, **80**, 148–157.
62. Schachtrup, C., Ryu, J.K., Helmrick, M.J., Vagena, E., Galanakis, D.K., Degen, J.L., Margolis, R.U. and Akassoglou, K. (2010) Fibrinogen triggers astrocyte scar formation by promoting the availability of active TGF-beta after vascular damage. *J. Neurosci.*, **30**, 5843–5854.
63. Previtali, S.C., Malaguti, M.C., Riva, N., Scarlato, M., Dacci, P., Dina, G., Triolo, D., Porrello, E., Lorenzetti, I., Fazio, R. *et al.* (2008) The extracellular matrix affects axonal regeneration in peripheral neuropathies. *Neurology*, **71**, 322–331.

64. Xu, P.T., Schmechel, D., Qiu, H.L., Herbstreith, M., Rothrock-Christian, T., Eyster, M., Roses, A.D. and Gilbert, J.R. (1999) Sialylated human apolipoprotein E (apoEs) is preferentially associated with neuron-enriched cultures from APOE transgenic mice. *Neurobiol. Dis.*, **6**, 63–75.
65. Murray, L.M., Lee, S., Baumer, D., Parson, S.H., Talbot, K. and Gillingwater, T.H. (2010) Pre-symptomatic development of lower motor neuron connectivity in a mouse model of severe spinal muscular atrophy. *Hum. Mol. Genet.*, **19**, 420–433.
66. Murray, L.M., Comley, L.H., Thomson, D., Parkinson, N., Talbot, K. and Gillingwater, T.H. (2008) Selective vulnerability of motor neurons and dissociation of pre- and post-synaptic pathology at the neuromuscular junction in mouse models of spinal muscular atrophy. *Hum. Mol. Genet.*, **17**, 949–962.
67. Murray, L.M., Thomson, D., Conklin, A., Wishart, T.M. and Gillingwater, T.H. (2008) Loss of translation elongation factor (eEF1A2) expression *in vivo* differentiates between Wallerian degeneration and dying-back neuronal pathology. *J. Anat.*, **213**, 633–645.
68. Murray, L.M., Talbot, K. and Gillingwater, T.H. (2010) Neuromuscular synaptic vulnerability in motor neuron disease; amyotrophic lateral sclerosis and spinal muscular atrophy. *Neuropathol. Appl. Neurobiol.*, **36**, 133–156.
69. Gillingwater, T.H., Thomson, D., Mack, T.G., Soffin, E.M., Mattison, R.J., Coleman, M.P. and Ribchester, R.R. (2002) Age-dependent synapse withdrawal at axotomised neuromuscular junctions in Wld(s) mutant and Ube4b/Nmnat transgenic mice. *J. Physiol.*, **543**, 739–755.
70. McLachlan, E.M. and Martin, A.R. (1981) Non-linear summation of end-plate potentials in the frog and mouse. *J. Physiol.*, **311**, 307–324.
71. Wishart, T.M., Paterson, J.M., Short, D.M., Meredith, S., Robertson, K.A., Sutherland, C., Cousin, M.A., Dutia, M.B. and Gillingwater, T.H. (2007) Differential proteomics analysis of synaptic proteins identifies potential cellular targets and protein mediators of synaptic neuroprotection conferred by the slow Wallerian degeneration (Wlds) gene. *Mol. Cell. Proteomics*, **6**, 1318–1330.
72. Wishart, T.M., Huang, J.P., Murray, L.M., Lamont, D.J., Mutsaers, C.A., Ross, J., Geldsetzer, P., Ansorge, O., Talbot, K., Parson, S.H. *et al.* (2010) SMN deficiency disrupts brain development in a mouse model of severe spinal muscular atrophy. *Hum. Mol. Genet.*, **19**, 4216–4228.
73. Comley, L.H., Wishart, T.M., Baxter, B., Murray, L.M., Nimmo, A., Thomson, D., Parson, S.H. and Gillingwater, T.H. (2011) Induction of cell stress in neurons from transgenic mice expressing yellow fluorescent protein: implications for neurodegeneration research. *PLoS ONE*, **6**, e17639.